

Polydopamine Nanoparticle-Coated Polysulfone Porous Granules as Adsorbents for Water Remediation

Tamara Posati,^{*,†} Morena Nocchetti,[‡] Alessandro Kovtun,[†] Anna Donnadio,[‡] Massimo Zambianchi,[†] Annalisa Aluigi,[†] Massimo L. Capobianco,[†] Franco Corticelli,[§] Vincenzo Palermo,^{†,¥} Giampiero Ruani,^{||} Roberto Zamboni,[†] Maria Luisa Navacchia,^{*,†} and Manuela Melucci^{*,†}

[†]Consiglio Nazionale delle Ricerche, Istituto per la Sintesi Organica e la Fotoreattività (CNR-ISOF), Via Piero Gobetti 101, 40129 Bologna, Italy

[‡]Dipartimento di Scienze Farmaceutiche, Università di Perugia, Via del Liceo, 1, 06123 Perugia, Italy

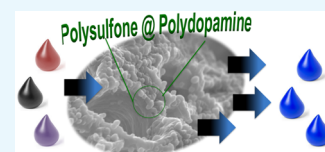
[§]Consiglio Nazionale delle Ricerche, Istituto di Microelettronica e Microsistemi (IMM-CNR), Via Piero Gobetti 101, 40129 Bologna, Italy

[¥]Department of Industrial and Materials Science, Chalmers University of Technology, Chalmersplatsen 4, 412 96 Göteborg, Sweden

^{||}Consiglio Nazionale delle Ricerche, Istituto per lo Studio dei Materiali Nanostrutturati (ISMN-CNR), Via Piero Gobetti 101, 40129 Bologna, Italy

Supporting Information

ABSTRACT: Water purification technologies possibly based on eco-sustainable, low cost, and multifunctional materials are being intensively pursued to resolve the current water scarcity and pollution. In this scenario, polysulfone hollow porous granules (PS-HPGs) prepared from scraps of the industrial production of polysulfone hollow fiber membranes were recently introduced as adsorbents and filtration materials for water and air treatment. Here, we report the functionalization of PS-HPGs with polydopamine (PD) nanoparticles for the preparation of a new versatile and efficient adsorbent material, namely, PSPD-HPGs. The in situ growth of PD under mild alkaline oxidative polymerization allowed us to stably graft PD on polysulfone granules. Enhanced removal efficiency of ofloxacin, an antibiotic drug, with an improvement up to 70% with respect to the pristine PS-HPGs, and removal of Zn(II) and Ni(II) were also observed after PD modification. Remarkably, removal of Cu(II) ions with an efficiency up to 80% was observed for PSPD-HPGs, whereas no adsorption was found for the PD-free precursor. Collectively, these data show that modification with a biocompatible polymer such as PD provides a simple and valuable tool to enlarge the field of application of polysulfone hollow granules for water remediation from both organic and metal cation contaminants.



INTRODUCTION

The development of advanced technologies for efficient water remediation is a matter of great current concern. Indeed, given the decreasing availability of fresh water all over the world and the increasing sources of water contamination, solutions for the simultaneous removal of different classes of pollutants, possibly based on environmentally sustainable and low-cost approaches are urgently required.¹ Adsorption on porous materials is one of the most simple and versatile strategies for water treatment;^{2–4} it is based on the chemi- or physisorption of adsorbate molecules on the adsorbent surface through cooperative intermolecular surface interactions that depend on the adsorbate and adsorbent nature. Activated carbons are the most commonly used adsorbent for the removal of organic microcontaminants,⁵ including those of emerging concern.⁶ However, despite their wide application range and low cost, they still suffer from expensive regeneration costs (both from energetic and environmental points of view) and loss of performance after regeneration.⁷ Materials alternative or complementary to activated carbons, including natural or plastic industrial wastes and nanomaterials, have been proposed.^{8–14} In this scenario, our group recently introduced

a new porous granular material, namely, polysulfone hollow porous granules (PS-HPGs, Figure 1), that allowed simultaneous adsorption of organic contaminants from water and gas phase and filtration of aerosol nano/microparticles.¹⁵ Interestingly, PS-HPGs were prepared by using scraps of polysulfone hollow fiber membranes derived from the production of commercial ultrafiltration modules. The industrial process employed for cartridge preparation leads to the production of scraps with an average amount of about 5–10% in weight of the total year production. We demonstrated that such scraps can be converted into a granular material (PS-HPGs) that preserves almost unchanged porosity and morphology (Figure 1b, right) of the starting hollow fibers but shows higher adsorption capability due to the higher surface area. Efficient removal of selected volatile organic compounds, polycyclic aromatic hydrocarbons, and emerging organic contaminants was demonstrated for PS-HPGs. In addition, filtration of aerosol particles was observed in dynamic experiments on in

Received: October 22, 2018

Accepted: December 14, 2018

Published: March 5, 2019

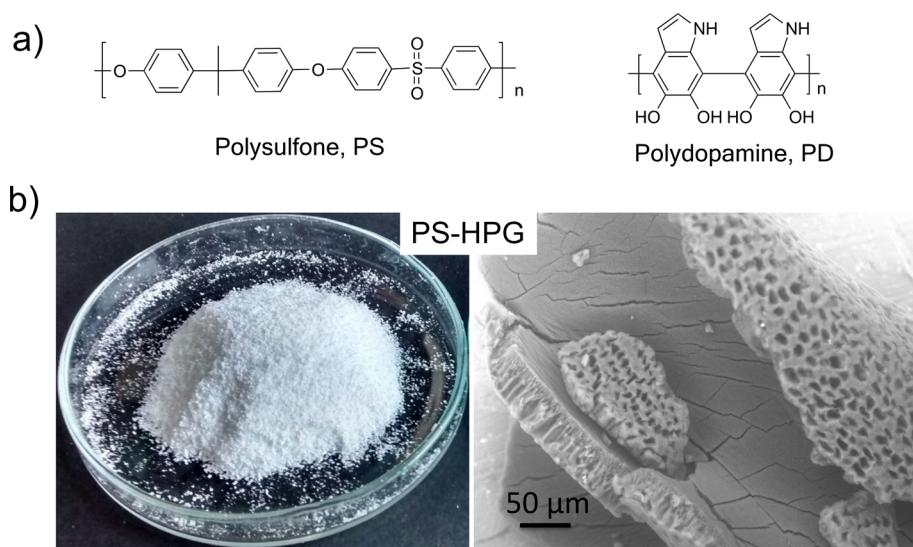


Figure 1. (a) Molecular structure of polysulfone and polydopamine. (b) Image of PS-HPG powder (left; photograph courtesy of “Mr. Massimo Zambianchi”, copyright 2016) and the structure observed by SEM analysis (right).¹⁵

situ-generated NaCl nanoparticles. Although filtration is enabled by the intrinsic porosity of the starting polysulfone membranes (Figure 1b, right), adsorption capability is related to the chemical structure of polysulfone and high surface area, allowing interactions with hydrophobic organic contaminants through secondary interactions. Aiming at the tailoring of the surface chemo–physical properties and at the consequent extension of the PS-HPG application range, we introduce here a polydopamine (PD; Figure 1a) nanoparticle-modified version of PS-HPGs, namely, PSPD-HPGs, which was prepared by in situ growth of polydopamine on polysulfone granule scaffolds. Polydopamine (PD) is a bioinspired melanin-like material that, because of its stability, biocompatibility, and easy deposition on many types of inorganic and organic substrates (ceramics, metals, oxides, synthetic, and natural polymers),^{16–18} has recently attracted much attention in several fields, such as medicine, energy, sensing, and water purification.^{19–22} The polydopamine structure includes catechol, amine, and imine functional groups (see Figure 1a).

In particular, catechol groups are crucial for the PD adhesion, which forms strong hydrogen bonds with the substrates onto which it is placed. Indeed, stable surface modification of filtration membranes with PD has been widely investigated to increase their hydrophilicity and, consequently, to improve their resistance to fouling during water filtration.²² In addition, the catechol groups and nitrogen heteroatoms are expected to be the active sites for heavy-metal ions, synthetic dyes, and other organic pollutants through electrostatic, bidentate chelating, or hydrogen-bonding interactions. In this respect, it has been recently demonstrated that PD coating increased the adsorption capacity of substrates on which it is deposited both in terms of organic contaminants and metal ions. For example, it has been demonstrated that the PD deposition on polysulfone membranes increased the removal of a representative positively charged contaminant as methylene blue (MB) with increasing PD coating time.²³ The increased removal of heavy metals and metal cations (i.e., Cd(II) and Pb(II)) upon PD functionalization of graphene hydrogel was also reported.²⁴ A similar behavior was also observed for PD-functionalized zeolite that showed an adsorption capacity toward Cu(II) at pH = 5.5, about 40% higher than that of the

pristine material.²⁵ On this basis, we envisioned the possibility of enhancing the adsorption versatility and efficiency of PS-HPGs by PD nanoparticle (NP) coating. Here, we demonstrated that in situ PD NPs adhere stably to PS-HPGs, affording a robust material able to remove both organic contaminants and metal ions from water. To test the absorption properties of PSPD-HPGs, we selected three different emerging organic contaminants (EOCs), suspected endocrine disruptors,^{26–28} such as Rhodamine B (RhB), a pink organic dye widely used in the textile industry, ofloxacin (OFLOX), an antibiotic found in influent waters and in sludge,²⁹ and benzophenone-4 (BP4), a bio-recalcitrant molecule widely used in sunscreen and found even in surface waters.³⁰ RhB was also chosen as a model organic micro-pollutant and is being already proven to be efficiently removed by PS-HPGs.³¹ Moreover, three bivalent metal cations such as Cu(II), Ni(II), and Zn(II) were also considered. Indeed, heavy metals generally derived from industrial wastewaters are also a matter of concern for their toxic effects on human health (high blood pressure, sleep disabilities, irritability, increased allergic reactions, etc.) that have been extensively investigated.^{32–34}

RESULTS AND DISCUSSION

Synthesis and Characterization. PS-HPGs coated with PD (PSPD-HPGs) were prepared by exploiting the oxidative polymerization of dopamine in alkaline aqueous solution (Figure 2a) (see Experimental Section). The color change of the PS-HPG material is the primary indicator of catechol oxidation and subsequent dopamine polymerization. Indeed, PS-HPGs (Figure 1b, left panel) appear white, whereas the PSPD-HPG-coated material displays a dark brownish color, which indicates the PD surface deposition (Figure 2b, right panel). After PD polymerization, the obtained PSPD-HPG material was collected, and before use, it was washed in flowing water, dried, and then rewashed with water to eliminate all the non-adsorbed PD (see Experimental Section). As indicated in Figure S1, the release of PD was completed after 4 h of washing, indicating that after this time, the material is ready to be used for absorption experiments without secondary contamination risks. The size and the surface charge of the NP-coating layer were characterized by dynamic light

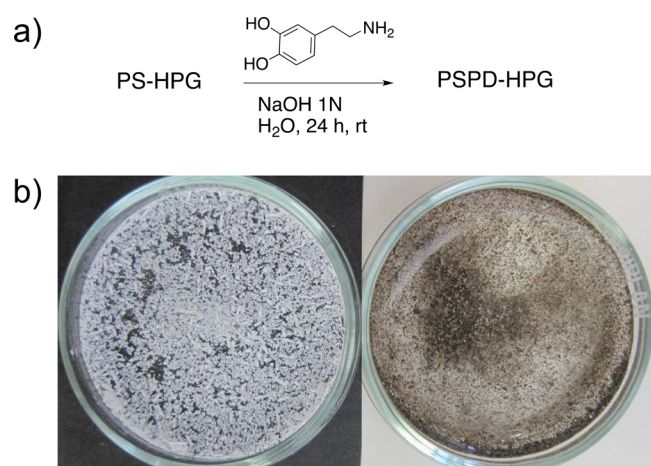


Figure 2. (a) Synthetic route to PSPD-HPGs. (b) Images of PS-HPGs (left) and PSPD-HPGs (right); the black color derived from the PD component (photograph courtesy of “Mr. Massimo Zambianchi”, copyright 2016).

scattering (DLS) and zeta potential (Pz) measurements on reference PD NPs prepared under the same experimental conditions (non-adsorbed). PD NPs showed a hydrodynamic diameter of 123.3 ± 4.4 nm and a Pz of -30.6 ± 1.4 mV. Finally, the amount of PD coating, calculated by elemental analysis (PS-HPGs: N = 0%; C = 52%; H = 2%; S = 6.2%; PSPD-HPGs: N = 0.58%; C = 70.40%; H = 4.81%; S = 7.20%), resulted in a weight percentage of PD in the PSPD-HPGs of around 6.1 wt %.

The morphology of the PSPD-HPG-coated material was investigated by SEM analysis. As showed in Figure 3, in

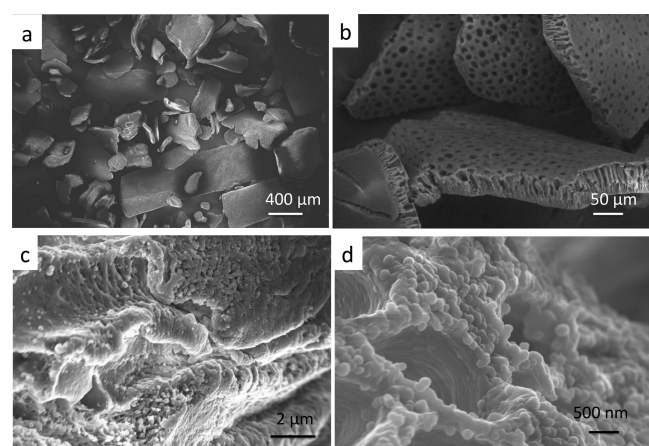


Figure 3. Structure of PSPD-HPGs at different magnifications observed by SEM. (a) Overall view of the granules. (b) Details of broken granules showing the porous surface and the section with the typical finger-like pores. (c) Detail of the pore channels coated with PD nanoparticles. (d) Detail of the PD NPs.

comparison to uncoated PS-HPGs,¹⁵ the PSPD-HPG material showed a very porous structure with the presence of a PD coating made of small particles with a mean diameter of about 130 nm in agreement with the DLS study (Figure 3c,d). The surface wettability of the PS-HPG and PSPD-HPG substrates was investigated by using contact angle measurements. Because the powders are not suitable for this type of measurements, the

same coating conditions were extended to PS membranes (Figure S2, Supporting Information).

Figure 4a,b shows the images of water droplets onto PS and PSPD membranes, respectively. The PS substrate shows a

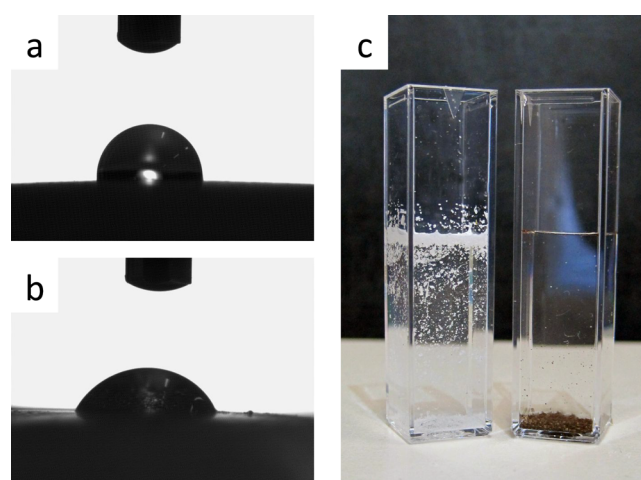


Figure 4. (a, b) Water contact angle experiment on (a) PS membrane and (b) PD nanoparticle-coated PS membrane. (c) Different behaviors of PS-HPGs (left) and PSPD-HPGs (right) in water (photograph courtesy of “Mr. Massimo Zambianchi”, copyright 2016).

contact angle value of about 93° (92.8 ± 2.7), whereas the PD-coated PS substrate displays a lower value of about 57° (57.4 ± 4.6), suggesting an increased wettability/hydrophilicity of the polysulfone after PD functionalization/coating. Pictures of the polysulfone granules dispersed in water are also reported (Figure 4c) to give an idea of the increased hydrophilicity of the PSPD-HPG material in comparison to uncoated PS-HPGs.

The structure of PS-HPGs after PD coating was investigated by ATR measurements. Figure 5 shows the ATR spectra of pristine PS-HPGs in comparison with PSPD-HPG-coated material. The spectra of PS-HPGs (black line) and PSPD-HPGs (red line) are very similar; however, the appearance of a broad background in the spectral region of C–C, C=C, and N–H vibrations in the PSPD-HPGs occurs, indicating the presence of a PD coating.^{19,35}

X-ray photoelectron spectroscopy (XPS) was used to study the surface chemistry of PSPD-HPGs, in relation with pristine polymers PD and PS-HPGs. The probe depth of XPS used in the experimental setup was about 3 nm. The stoichiometric ratios are reported in Table 1, and the S 2p and N 1s spectra are shown in Figure 6. The PS-HPG spectrum was in excellent agreement with previously published data; particularly, the binding energy of S 2p_{3/2} was 168.0 ± 0.1 eV (see Figure 6), corresponding to the R2–SO₂ group of PS,³⁶ and the stoichiometry ratios of O/C and S/C in Table 1 have confirmed the chemical structure in Figure 1a. The PD powder has the expected stoichiometry for O/C and N/C ratios; moreover, the N 1s peak (400.2 ± 0.1 eV) was associated to the amine group (R–NH–R)³⁷ present in the PD chemical structure in Figure 1a. The N 1s and the S 2p signals were univocally associated with the PD and PS-HPGs, respectively; thus, in the first approximation, it was possible to quantify the amount of PD coating on the PSPD-HPGs, which presents both of these XPS peaks (Figure 6), as the ratio between the area of N 1s peak over the sum of the areas of N 1s and S 2p

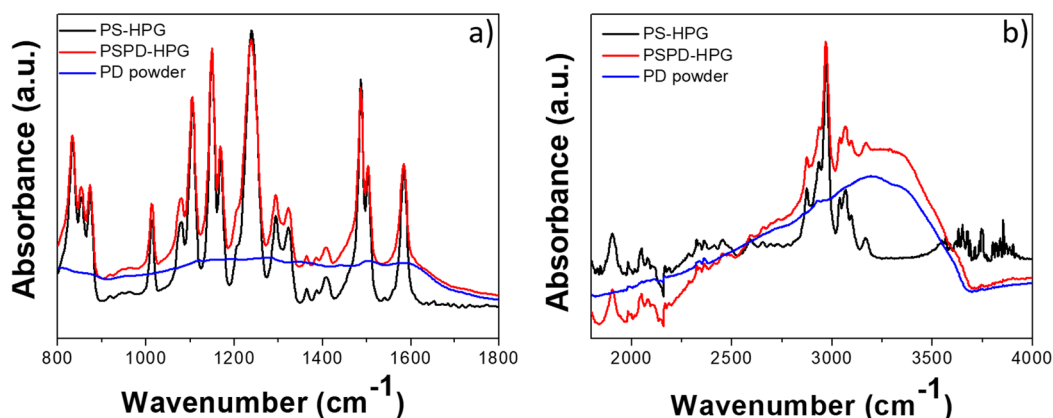


Figure 5. (a, b) ATR adsorption spectra of PS-HPGs (black line), PSPD-HPGs (red line), and PD (blue line) in the (a) 800–1800 cm^{-1} and (b) 1800–4000 cm^{-1} regions.

Table 1. Stoichiometric Ratios Measured by XPS for PS-HPGs, PD powder, and PSPD-HPGs

sample	O/C	N/C	S/C
PS-HPGs	0.13 ± 0.01 (0.15^a)		0.04 ± 0.01 (0.04^a)
PD powder	0.28 ± 0.02 (0.25^b)	0.12 ± 0.01 (0.13^b)	
PSPD-HPGs	0.28 ± 0.02	0.10 ± 0.01	0.004 ± 0.001

^aExpected values for PS. ^bExpected values for PD.

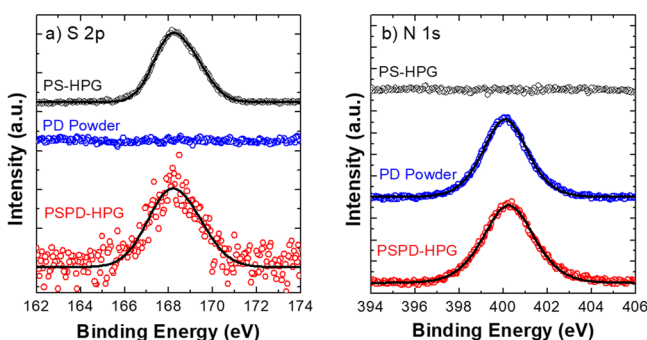


Figure 6. (a) XPS S 2p of PS-HPGs (black), PD powder (blue), and PSPD-HPGs (red). (b) XPS N 1s of PS-HPGs (black), PD powder (blue), and PSPD-HPGs (red). All spectra are normalized.

peaks. The S 2p peak in PSPD-HPGs was 10 times less intense than that in the pristine PS-HPGs (S/C goes from 0.04 ± 0.01 in PS-HPGs to 0.004 ± 0.001 in PSPD-HPGs); thus, the obtained PD coverage was significantly high ($96 \pm 2\%$). No chemical shift was observed in the S 2p and N 1s of the PSPD-HPGs with respect to the pristine polymers. Resuming, the ATR elemental analysis and XPS confirmed that the homogeneous nanoparticle coating observed by SEM analysis is made of PD.

Adsorption Experiments. EDC Adsorption Test. The adsorption experiments were performed in batch at three different contact times (15 min, 1 h, and 24 h) (Figure 7) using an adsorbate initial concentration of 5 mg/L of each compound and an adsorbent dosage of 2 g/L. After 15 min treatment, PSPD-HPGs work more efficiently than PS-HPGs for OFLOX, whereas BP4 and RhB were more efficiently captured by PS-HPGs. The same trend was observed at a treatment time of 1 h with a slight increase in the removal efficiency of PSPD-HPGs ($52\% \rightarrow 59\%$ for OFLOX and $50\% \rightarrow 66\%$ for RhB). However, upon increasing the treatment time to 24 h (Figure 7), the OFLOX removal efficiency of

PSPD-HPGs was even superior than that of PS-HPGs (81% vs 47%), whereas the RhB removal was the similar to that of PS-HPGs (99% vs 99%). BP4 was poorly removed by both materials with similar performances (9% vs 10%). These data suggest a slower kinetics for PSPD-HPGs but an almost competitive or even better performance in the case of OFLOX once equilibrium is reached. OFLOX and BP4 have similar molecular weight, solubility, and $\log K_{ow}$ (Table S1, Supporting Information). However, only for OFLOX, a 1.7-fold increase in removal (corresponding to 72% improvement) was observed for PSPD-HPGs with respect to PS-HPGs. No improvement after PD coating was found for BP4 (removal of $<10\%$). The removal improvement in the case of OFLOX together with the lack of effect for BP4 could be thus related to the strongly different dipole moments of the two molecules (Table S1 and Figure S3, Supporting Information). Indeed, OFLOX with a dipole moment of 13.0 debye is removed better than BP4, for which a lower value up to 5.9 debye is reported. In turn, the PS-HPG functionalization with PD increases the presence of polar groups on the surface, thereby enhancing the dipole–dipole interactions that can promote the adsorption of the more polar OFLOX compared to BP4. In agreement, a similar behavior was observed for polysulfone–graphene oxide (PS-GO) composite with respect to GO-free counterparts, in which the higher hydrophilicity of GO increases the interactions with polar compounds.³¹

Metal Cations. The pH of the solution has an important effect on the adsorption process as it influences the structure of the adsorbent and the metal ion speciation in solution. The studies on the effects of pH were carried out in the pH range of 2.0–6.0, according to the stability of each metal ion. Figure 8a shows the metal ion removal efficiency of PSPD-HPGs as a function of solution pH. From Figure 8a, an increase in the metal ions adsorbed has been observed with the increasing pH. In particular, the amount of metal ions adsorbed increased until pH 4.0 for Cu(II) and until pH 6.0 for Zn(II) and Ni(II). In acidic solutions (pH values lower than 3.0), the protonation

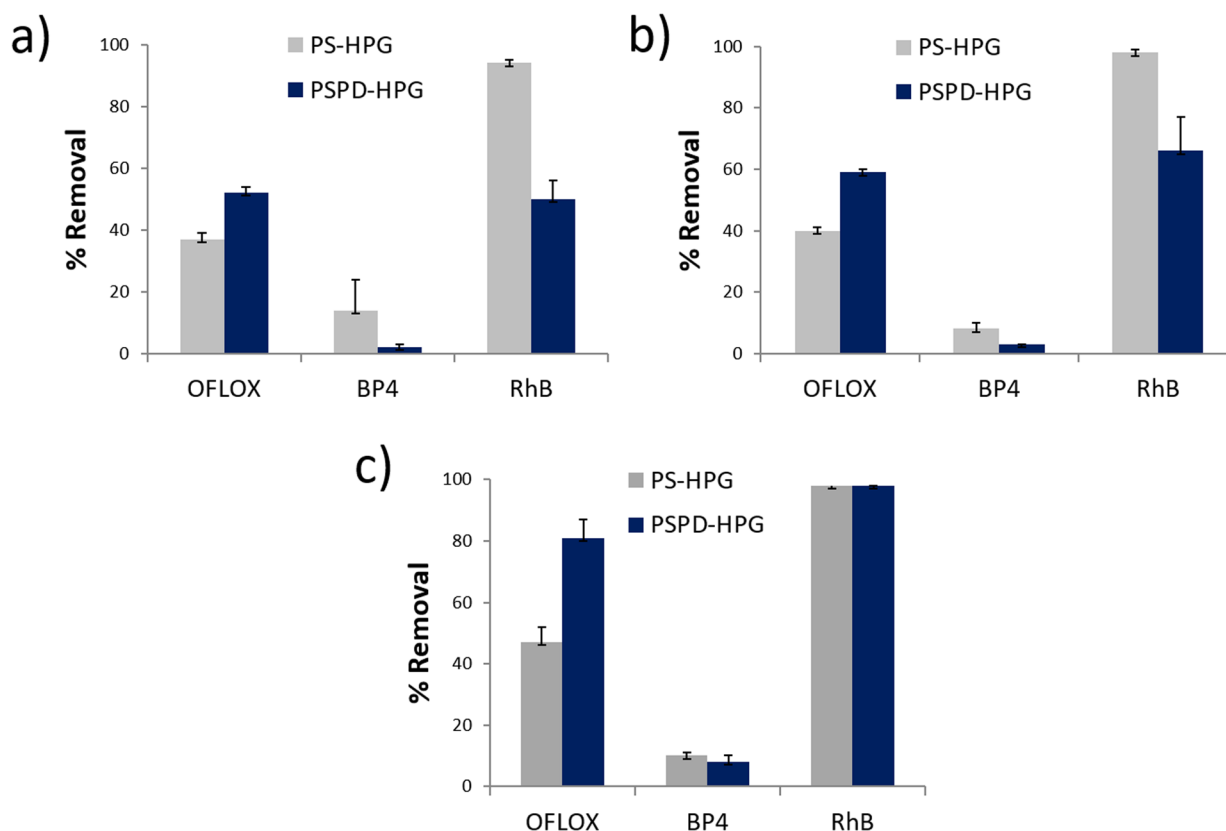


Figure 7. (a–c) Adsorption of EDCs by PS-HPGs and PSPD-HPGs at different treatment times: (a) 15 min, (b) 1 h, and (c) 24 h. The adsorption experiments were performed in batch using 50 mg of PSPD-HPGs in 25 mL of EDC solution (5 mg/L of each compound).

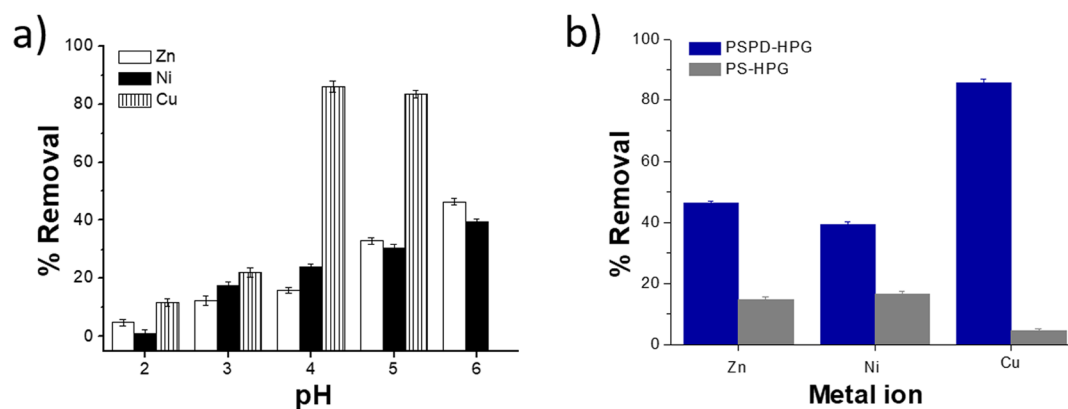


Figure 8. (a) Percentage of removal of the indicated metal ions by PSPD-HPGs as a function of pH. (b) Comparison between the % of removal of the indicated metal ions by PS-HPGs and PSPD-HPGs at the optimum pH of adsorption.

of chemical functional groups on PSPD-HPGs resulted in a positively charged surface; as a consequence, the adsorption capacities of metal ions were low due to the electrostatic repulsion. With increasing pH values, the surface charges of PSPD-HPGs became more negative, and the adsorption capacities of Zn(II), Ni(II), and Cu(II) increased in the range of pH values from 3.0 to 6.0. For pH = 5, the adsorption ability of Cu(II) was decreased probably due to the formation of metal hydroxide adducts resulting in reduced activity of metal ions in solution; for pH > 6, the precipitation of Cu(OH)₂ colloidal particles increases, and the data are not comparable with those obtained at lower pH.³⁸ The optimum pH for the adsorption of Zn(II), Ni(II), and Cu(II) was then recorded at pH 6.0, 6.0, and 4.0, respectively. As shown in

Figure 8b, under these pH conditions, the metal ion uptake of uncoated PS-HPGs was very low; in particular, it was negligible for Cu(II), indicating that, in this case, the uptake can be ascribed only to the PD deposited on the polymer. Because the best performances of PSPD-HPGs were observed for copper ions (almost 90% of removal efficiency), we focused our work on this type of metal ion. The Cu(II) adsorption isotherm of PSPD-HPGs was then obtained at the optimum adsorption pH, equilibrating, at room temperature and for 24 h, the sorbent (2 g/L) with copper solutions having concentrations ranging from 1 to 300 mg/L. To analyze the phenomenon of metal ion release from the PSPD-HPGs_Cu, release tests were obtained by contacting the PSPD-HPGs_Cu with aqueous solution and HCl solution. Thus, we analyzed the supernatant

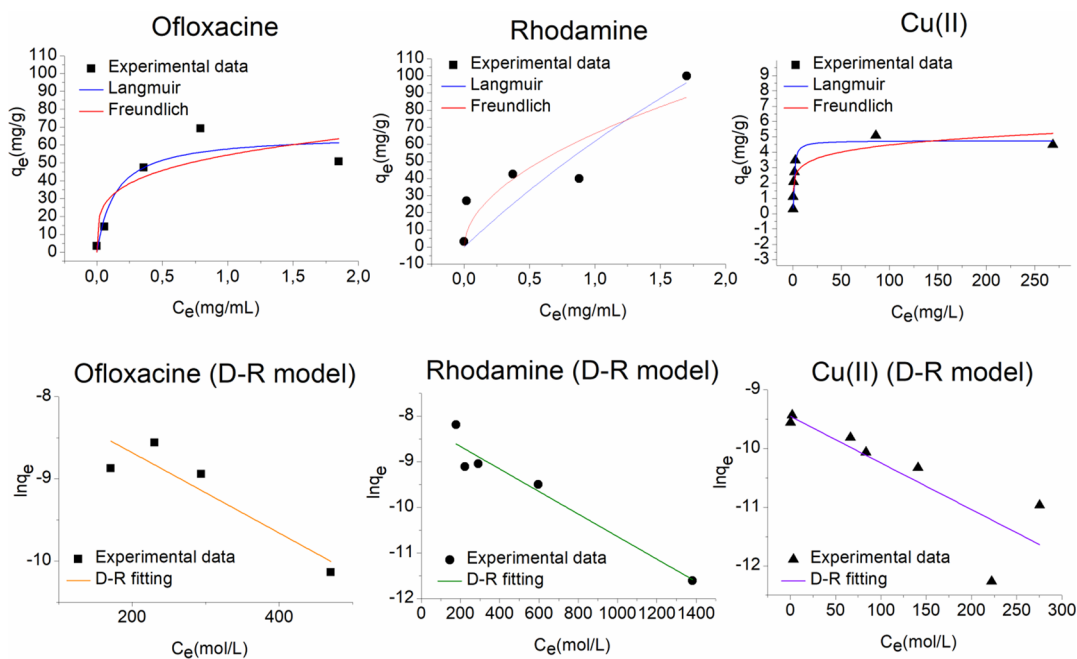
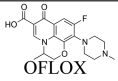
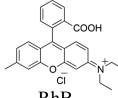
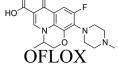
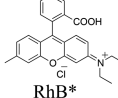


Figure 9. Plots of the fitting of the experimental data with Langmuir, Freundlich, BET, and Dubinin–Radushkevich for RhB and OFLOX. Adsorption isotherm at 20 °C, pH = 7, and contact time = 24 h (25 mg of adsorbent PSPD-HPGs, volume of 4 mL, C_0 of 4–0.01 mg/mL for RhB and 2–0.01 mg/mL for OFLOX).

Table 2. Adsorption Isotherm Parameters

Adsorbent	Adsorbate	LANGMUIR			FREUNDLICH			Dubinin–Radushkevich		
		q_m (mg/g)	K_L (L/g)	R^2	K_F	n	R^2	q_s (mol/g)	E (KJ/mol)	R^2
PSPD-HPG	 OFLOX	66±11	7.1±0.2	0.885	54±9	6±4	0.698	$(5±2) \times 10^{-5}$	10±2	0.749
	 RhB	456±1394	0.26±0.6	0.678	66±10	2±1	0.736	$(2.9±0.6) \times 10^{-4}$	14±1	0.925
	Cu(II)	4.8±0.3	1.1±0.3	0.927	2.2±0.4	7±2	0.734	$(8±3) \times 10^{-5}$	8±1	0.662
PS-HPG	 OFLOX	24±3	9±1	0.805	9.9±0.1	6.4±0.8	0.99656	$(1.5±0.1) \times 10^{-4}$	8±2	0.991
	 RhB*	22±2	9±6	0.805	17±1	4.4±0.7	0.923	$(8±1) \times 10^{-5}$	14±1	0.908

after the filtration of PSPD-HPGs_Cu immersed in acidic and aqueous media. The copper release in an acidic environment was almost complete, whereas that in bidistilled water was around 1.7%, demonstrating that the PSPD-HPGs_Cu complex is stable in water, and at the same time, the sorbent can be regenerated after acidic treatment.

Nonlinear Fitting of the Isotherm Models. The mechanism of adsorption of PSPD-HPGs was studied through adsorption isotherms and compared with that of starting PS-HPGs. Langmuir, Freundlich, and Dubinin–Radushkevich adsorption isotherms for RhB, OFLOX, and Cu(II), respectively, are shown in Figure 9, whereas the corresponding correlation coefficients, isotherm parameters, and related standard deviations are reported in Table 2. For the PS-HPG sample,

only the experimental data related to the adsorption of OFLOX and RhB were considered, because that sample showed nonsignificant adsorption toward Cu(II) cations. OFLOX is a neutral polar and hydrophilic molecule ($\log K_{ow} = -0.4$), and RhB is a zwitterion (physicochemical properties shown in Table S1, Supporting Information). The adsorption of RhB from both PS-HPGs and PSPD-HPGs is very high, whereas OFLOX is better adsorbed by PSPD-HPGs than PS-HPGs. For all these reasons, we considered them for the mechanism insight. Langmuir isotherm is an empirical model, which assumes that the adsorption is a monolayer adsorption occurring at a finite number of localized sites.³⁹ The expression of Langmuir isotherm model is illustrated by the following equation

$$q_e = q_m K_L \frac{C_e}{1 + K_L C_e} \quad (1)$$

where C_e (mg/L) is the concentration of the adsorbate at equilibrium, q_e (mg/g) is the corresponding adsorption capacity, and q_m (mg/g) and K_L (L/mg) are related to the adsorption capacity and net enthalpy of adsorption, respectively. Freundlich adsorption describes the non-ideal and reversible adsorption, which can be applied to multilayer adsorption, on the basis of an assumption concerning the energetic surface heterogeneity.⁴⁰ The nonlinear equation of the Freundlich isotherm model is illustrated by the equation

$$q_e = K_F C_e^{1/n} \quad (2)$$

where K_F and n are the constants that measure the adsorption capacity and surface heterogeneity, respectively. In particular, the smaller $1/n$, the greater the expected heterogeneity. If n lies between 1 and 10, this indicates a favorable sorption process. The Dubinin–Radushkevich (D-R)⁴¹ isotherm is another empirical model generally applied to describe the adsorption process onto both homogeneous and heterogeneous surfaces. The linear expression of the D-R model is described by eqs 3 and 4

$$\ln q_e = \ln q_s - K_D \varepsilon^2 \quad (3)$$

$$\varepsilon = RT \ln \left(1 + \frac{1}{C_e} \right) \quad (4)$$

where q_s (mol/g) is related to the adsorption capacity, K_D (mol^2/kJ^2) is a constant related to the mean free energy of adsorption R (J/mol·K), which is the gas constant, and T (K) is the absolute temperature. The mean free energy E (kJ/mol) can be calculated by using the following equation:

$$E = \frac{1}{\sqrt[3]{2K_D}} \quad (5)$$

The E value gives information about the adsorption mechanism: if the magnitude of E is between 8 and 16 kJ/mol, the adsorption process is of chemical type, whereas when $E < 8$ kJ/mol, the adsorption process proceeds physically.⁴² As a concern to the OFLOX adsorption on PSPD-HPGs, the highest R^2 value and the lowest standard deviations were derived by fitting the experimental data with the Langmuir isotherm model, thereby suggesting a monolayer adsorption where the estimated maximum adsorption capacity is 66 mg/g. The E value obtained from the fitting with the D-R model falls between 8 and 16 kJ/mol, indicating an adsorption mechanism of chemical type (i.e., through van der Waals and H-bond interactions). The functionalization of polysulfone with dopamine modifies the adsorption behavior of the material toward OFLOX. Indeed, the OFLOX adsorption on PS-HPGs is better fitted by the Freundlich model, indicating a multilayer adsorption on a heterogeneous surface. Moreover, the energy of adsorption calculated by the D-R model is 8, indicating predominant physical interactions between the adsorbent and the adsorbate. Meanwhile, the fitting of the experimental data related to the adsorption of RhB on PSPD-HPGs results in a higher R^2 value and lower standard deviations for the Freundlich model, compared to the Langmuir model, indicating a multilayer adsorption of RhB onto the adsorbent surface. Moreover, the n value lies between 1 and 10, indicating a favorable adsorption. Also, in this case, the mean free energy

of adsorption falls between 8 and 16 kJ/mol, indicating a chemical-type adsorption (likely an interplay of π - π stacking and electrostatic interactions). Moreover, the obtained E value is higher for RhB than OFLOX, suggesting stronger chemical interactions of the adsorbent with RhB than those occurring with OFLOX. Also, the RhB adsorption on PS-HPGs is a favorable adsorption, which follows the Freundlich model ($n < 10$); however, the K_F value calculated for the PSPD-HPG adsorbent is about four times higher than that of PS-HPGs, demonstrating that the functionalization of PS with PD increases the adsorption performances of the material toward the RhB. The best fitting for the Cu(II) adsorption is given by the Langmuir isotherm model, and the calculated theoretical value for the maximum adsorption capacity is 4.8 mg/g. In this case, the mean free energy calculated through the D-R model is 8 kJ/mol, suggesting a physical-type adsorption of copper ions onto the adsorbent surface.

CONCLUSIONS

In conclusion, we demonstrated that polysulfone granules prepared by using industrial scraps of polysulfone hollow fiber membranes (PS-HPGs) can be efficiently coated with PD nanoparticles to provide an eco-sustainable and low-cost material to be used as adsorbents for drinking water treatment. Simultaneous adsorption of organic and metal ions contaminants from water was indeed achieved only after PD functionalization with removal capabilities of PSPD-HPGs toward OFLOX, RhB, and Cu(II) consistently enhanced compared to that of uncoated PS-HPGs. Synergic chemical and physical adsorption mechanisms of removal of the targeted contaminants were allowed by PD functionalization; indeed, physical adsorption mechanism was evidenced by the D-R model for Cu(II) adsorption only for PSPD-HPGs. Notably, the porosity of the PS hollow granule derived from the industrial polysulfone hollow fiber ultrafiltration membranes is retained after chemical modification, suggesting the possibility to exploit PSPD-HPGs for combined adsorption and filtration purposes. Studies in this direction are currently underway.

EXPERIMENTAL SECTION

PSPD-HPG Synthesis. The PD coating on PS-HPGs was performed by exploiting the oxidative polymerization of dopamine in aqueous solution.⁴³ Specifically, 5 g of polysulfone granules was added to 0.01 M dopamine hydrochloride aqueous solution. A solution of 1 N NaOH (molar ratio of dopamine hydrochloride to NaOH, 1:1) was added to the dopamine hydrochloride solution at room temperature under vigorous stirring. The white granules rapidly turned pale yellow and then gradually changed to dark brown. The polymerization was carried out for 24 h (shorter polymerization times such as 5 h lead to unstable coating and significant NP release), and after aging, the PSPD-HPGs were recovered by filtration and washed in a flowing water (1 L of deionized water for 1 g of the PSPD-HPG material) for 1 h. The obtained PSPD-HPG material was then dried at 50 °C until a constant weight and rewashed with water before use for 5 h to remove all the unabsorbed PD (see Figure S1, Supporting Information).

Characterization. Carbon, nitrogen, and hydrogen contents were determined by elemental analysis using an EA 1108 CHN Fisons instrument. The zeta potential (Pz) and dynamic light scattering (DLS) measurements on PD NPs in water

solution were performed by a NanoBrook Omni Particle Size Analyzer (Brookhaven Instruments Corporation, USA) equipped with a 35 mW red diode laser (nominal 640 nm wavelength). ATR spectra ($380\text{--}4000\text{ cm}^{-1}$) of PD, PS-HPG, and PSPD-HPG materials were performed by means of an FT-IR Bruker Vertex 70 interferometer equipped with a diamond crystal single reflection Platinum ATR accessory. The curve fitting was performed by using the Levenberg–Marquardt algorithm implemented in the OPUS 2.0 software. PSPD-HPGs were imaged with SEM (ZEISS LEO 1530 FEG) after metallization with gold. The high-resolution XPS spectra were recorded with a Phoibos 100 hemispherical energy analyzer (Specs) using Mg K α radiation ($\hbar\omega = 1253.6\text{ eV}$; X-ray power = 125 W) in a constant analyzer energy (CAE) mode, with analyzer pass energies of 40 eV. The base pressure in the analysis chamber during analysis was 1×10^{-9} mbar. All spectra were calibrated to the C 1s binding energy (285.0 eV). Spectra were fitted by using CasaXPS (www.casaxps.com). The N 1s peak was fitted by using a single Voigt curve, whereas the S 2p doublet with 2 Voigt curves (S 2p $_{3/2}$ and S 2p $_{1/2}$) with a constrained area ratio (2:1) and spin–orbit split S 2p $_{1/2}$ – S 2p $_{3/2} = 1.18\text{ eV}$. Water contact angles were measured by the static sessile drop method using a Digidrop GBX Model DS. For each film, at least five drops were measured. The water droplets used for the measurements had a volume of 1 μL .

Adsorption Tests. Metal analyses were performed by Varian 700-ES series inductively coupled plasma–optical emission spectrometers (ICP-OES). Standard solutions of 5 ppm containing Cu at pH values of 2, 3, 4, and 5 were prepared by adding a proper amount of 0.1 M HCl or 0.1 M NaOH by means of an automatic titrator. The effect of pH on Cu(II) adsorption was evaluated by suspending 15 mg of PSPD-HPGs in 7.5 ml of metal standard solutions for 24 h at room temperature. The suspensions were filtrated, and the mother waters were recovered and analyzed for the metal content. The copper uptake curve was also obtained by equilibrating 15 mg of PSPD-HPGs in 7.5 ml of metal standard solutions having concentrations ranging from 1 to 300 ppm for 24 h at room temperature. For release tests, 25 mg of PSPD-HPGs_Cu was suspended in 12.5 mL of 0.1 M HCl, and the same amount was suspended in 12.5 mL of ultrapure water at room temperature. After 24 h, the solutions were separated by filtration from the solids and submitted to ICP analysis. All assays were performed in triplicate, and the mean values were reported. Data processing was carried out with the ORIGIN 8.1 software (OriginLab Corporation, MA, USA). EOC adsorption was performed by using 50 mg of adsorbent in 25 mL of EOC solution (5 mg/L of each compound). EOC analyses were performed by HPLC (Agilent Technologies, 1260 Infinity equipped with a variable wavelength detector) via an optimized method using a C-8 analytical column (Agilent XDB-C8, $4.6 \times 50\text{ mm}$) and Milli-Q water/0.05% trifluoroacetic acid (mobile phase A) and acetonitrile (mobile phase B) at a flow rate of 1 mL/min. A linear gradient progressed from 20% B (initial conditions) to 100% B was used. The UV detection of each compound was done at λ_{max} (296 nm for OFLOX, 282 nm for BP-4, and 540 nm for RhB). The efficiencies reported in Figure 7 are the average value of three independent experiments (\pm SD).

Adsorption Isotherm Modeling. The amount of the contaminants adsorbed at equilibrium was calculated by the equation

$$q = \frac{(C_0 - C_e) \times V}{m}$$

where C_0 and C_e are the initial and equilibrium adsorbate concentrations (mg/L), respectively, V (L) is the volume of the solution, and m (g) is the mass of the adsorbent. All the adsorption isotherm data were used for modeling. In particular, three nonlinear isotherm models, namely, Langmuir, Freundlich, and Dubinin–Radushkevich, were employed to correlate the experimental data. To determine the best fit, the correlation coefficient (R^2) and the standard deviation (\pm SD) for each parameter were used to evaluate the data.

■ ASSOCIATED CONTENT

📄 Supporting Information

The Supporting Information is available free of charge on the ACS Publications website at DOI: [10.1021/acsomega.8b02900](https://doi.org/10.1021/acsomega.8b02900).

Polydopamine release test, control membranes synthesis, physicochemical properties of RhB, OFLOX, and BP4, and removal improvement of PSPD-HPGs over PS-HPGs (PDF)

■ AUTHOR INFORMATION

Corresponding Authors

*E-mail: tamara.posati@isof.cnr.it (T.P.).

*E-mail: marialuisa.navacchia@isof.cnr.it (M.L.N.).

*E-mail: manuela.melucci@isof.cnr.it (M.M.).

ORCID

Tamara Posati: 0000-0002-3879-266X

Anna Donnadio: 0000-0003-2903-4135

Massimo L. Capobianco: 0000-0002-4237-1198

Giampiero Ruani: 0000-0001-9326-0490

Maria Luisa Navacchia: 0000-0001-7175-1504

Author Contributions

The manuscript was written through the contributions of all authors. All authors have given approval to the final version of the manuscript.

Notes

The authors declare no competing financial interest.

■ ACKNOWLEDGMENTS

We thank L. Bocchi and M. Fecondini of Medica group for kindly providing us polysulfone hollow fibers and their scraps of production.

■ REFERENCES

- (1) Shannon, M. A.; Bohn, P. W.; Elimelech, M.; Georgiadis, J. G.; Mariñas, B. J.; Mayes, A. M. Science and technology for water purification in the coming decades. *Nature* **2008**, *452*, 301–310.
- (2) Alonso, A.; Moral-Vico, J.; Abo Markeb, A.; Busquets-Fité, M.; Komilis, D.; Puentes, V.; Sánchez, A.; Font, X. Critical review of existing nanomaterial adsorbents to capture carbon dioxide and methane. *Sci. Total Environ.* **2017**, *595*, 51–62.
- (3) Alsbaiee, A.; Smith, B. J.; Xiao, L.; Ling, Y.; Helbling, D. E.; Dichtel, W. R. Rapid removal of organic micropollutants from water by a porous β -cyclodextrin polymer. *Nature* **2016**, *529*, 190–194.
- (4) Jiang, N.; Shang, R.; Heijman, S. G. J.; Rietveld, L. C. High-silica zeolites for adsorption of organic micro-pollutants in water treatment: A review. *Water Res.* **2018**, *144*, 145–161.
- (5) Bansal, R. C.; Goyal, M. *Activated Carbon Adsorption*, 1st ed.; CRC: Boca Raton, FL, 2005; chapters 1–8.

- (6) Delgado, L. F.; Charles, P.; Glucina, K.; Morlay, C. The removal of endocrine disrupting compounds, pharmaceutically activated compounds and cyanobacterial toxins during drinking water preparation using activated carbon—A review. *Sci. Total Environ.* **2012**, *435–436*, 509–525.
- (7) Martin, R. J.; Ng, W. J. Chemical regeneration of exhausted activated carbon—I. *Water Res.* **1984**, *18*, 59–73.
- (8) Sud, D.; Mahajan, G.; Kaur, M. P. Agricultural waste material as potential adsorbent for sequestering heavy metal ions from aqueous solutions – A review. *Bioresour. Technol.* **2008**, *99*, 6017–6027.
- (9) Bhatnagar, A.; Sillanpää, M. Utilization of agro-industrial and municipal waste materials as potential adsorbents for water treatment—A review. *Chem. Eng. J.* **2010**, *157*, 277–296.
- (10) Ali, I. New Generation Adsorbents for Water Treatment. *Chem. Rev.* **2012**, *112*, 5073–5091.
- (11) Gupta, V. K.; Suhas. Application of low-cost adsorbents for dye removal – A review. *J. Environ. Manage.* **2009**, *90*, 2313–2342.
- (12) Perreault, F.; Fonseca de Faria, A.; Elimelech, M. Environmental applications of graphene-based nanomaterials. *Chem. Soc. Rev.* **2015**, *44*, 5861–5896.
- (13) Santhosh, C.; Velmurugan, V.; Jacob, G.; Jeong, S. K.; Grace, A. N.; Bhatnagar, A. Role of nanomaterials in water treatment applications: A review. *Chem. Eng. J.* **2016**, *306*, 1116–1137.
- (14) Lata, S.; Samadder, S. R. Removal of arsenic from water using nano adsorbents and challenges: A review. *J. Environ. Manage.* **2016**, *166*, 387–406.
- (15) Zambianchi, M.; Aluigi, A.; Capobianco, M. L.; Corticelli, F.; Elmi, L.; Zampolli, S.; Stante, F.; Bocchi, L.; Belosi, F.; Navacchia, M. L.; Melucci, M. Polysulfone Hollow Porous Granules Prepared from Wastes of Ultrafiltration Membranes as Sustainable Adsorbent for Water and Air Remediation. *Adv. Sustainable Syst.* **2017**, *1*, 1700019.
- (16) Thakur, V. K.; Vennerberg, D.; Kessler, M. R. Green Aqueous Surface Modification of Polypropylene for Novel Polymer Nanocomposites. *ACS Appl. Mater. Interfaces* **2014**, *6*, 9349–9356.
- (17) Hu, M.; Mi, B. Enabling Graphene Oxide Nanosheets as Water Separation Membranes. *Environ. Sci. Technol.* **2013**, *47*, 3715–3723.
- (18) Posati, T.; Ferroni, C.; Aluigi, A.; Guerrini, A.; Rossi, F.; Tatini, F.; Ratto, F.; Marras, E.; Gariboldi, M. B.; Sagnella, A.; Ruani, G.; Zamboni, R.; Varchi, G.; Sotgiu, G. Mild and Effective Polymerization of Dopamine on Keratin Films for Innovative Photoactivable and Biocompatible Coated Materials. *Macromol. Mater. Eng.* **2018**, *303*, 1700653.
- (19) Posati, T.; Sotgiu, G.; Varchi, G.; Ferroni, C.; Zamboni, R.; Corticelli, F.; Puglia, D.; Torre, L.; Terenzi, A.; Aluigi, A. Developing keratin sponges with tunable morphologies and controlled antioxidant properties induced by doping with polydopamine (PDA) nanoparticles. *Mater. Des.* **2016**, *110*, 475–484.
- (20) Madhurakkat Perikamana, S. K.; Lee, J.; Lee, Y. B.; Shin, Y. M.; Lee, E. J.; Mikos, A. G.; Shin, H. Materials from Mussel-Inspired Chemistry for Cell and Tissue Engineering Applications. *Biomacromolecules* **2015**, *16*, 2541–2555.
- (21) Liu, Y.; Ai, K.; Lu, L. Polydopamine and Its Derivative Materials: Synthesis and Promising Applications in Energy, Environmental, and Biomedical Fields. *Chem. Rev.* **2014**, *114*, 5057–5115.
- (22) Miller, D. J.; Dreyer, D. R.; Bielawski, C. W.; Paul, D. R.; Freeman, B. D. Surface Modification of Water Purification Membranes. *Angew. Chem., Int. Ed.* **2017**, *56*, 4662–4711.
- (23) Capozzi, L. C.; Mehmood, F. M.; Giagnorio, M.; Tiraferri, A.; Cerruti, M.; Sangermano, M. Ultrafiltration Membranes Functionalized with Polydopamine with Enhanced Contaminant Removal by Adsorption. *Macromol. Mater. Eng.* **2017**, *302*, 1600481.
- (24) Gao, H.; Sun, Y.; Zhou, J.; Xu, R.; Duan, H. Mussel-Inspired Synthesis of Polydopamine-Functionalized Graphene Hydrogel as Reusable Adsorbents for Water Purification. *ACS Appl. Mater. Interfaces* **2013**, *5*, 425–432.
- (25) Yu, Y.; Shapter, J. G.; Popelka-Filcoff, R.; Bennett, J. W.; Ellis, A. V. Copper removal using bio-inspired polydopamine coated natural zeolites. *J. Hazard. Mater.* **2014**, *273*, 174–182.
- (26) Petrie, B.; Barden, R.; Kasprzyk-Hordern, B. A review on emerging contaminants in wastewaters and the environment: Current knowledge, understudied areas and recommendations for future monitoring. *Water Res.* **2015**, *72*, 3–27.
- (27) Ternes, T.; Joss, A.; Oehlmann, J. Occurrence, fate, removal and assessment of emerging contaminants in water in the water cycle (from wastewater to drinking water). *Water Res.* **2015**, *72*, 1–2.
- (28) Muruganathan, M.; Yoshihara, S.; Rakuma, T.; Shirakashi, T. Mineralization of bisphenol A (BPA) by anodic oxidation with boron-doped diamond (BDD) electrode. *J. Hazard. Mater.* **2008**, *154*, 213–220.
- (29) Santos, L. H. M. L. M.; Araújo, A. N.; Fachini, A.; Pena, A.; Delerue-Matos, C.; Montenegro, M. C. B. S. M. Ecotoxicological aspects related to the presence of pharmaceuticals in the aquatic environment. *J. Hazard. Mater.* **2010**, *175*, 45–95.
- (30) Kasprzyk-Hordern, B.; Dinsdale, R. M.; Guwy, A. J. The removal of pharmaceuticals, personal care products, endocrine disruptors and illicit drugs during wastewater treatment and its impact on the quality of receiving waters. *Water Res.* **2009**, *43*, 363–380.
- (31) Zambianchi, M.; Durso, M.; Liscio, A.; Treossi, E.; Bettini, C.; Capobianco, M. L.; Aluigi, A.; Kovtun, A.; Ruani, G.; Corticelli, F.; Brucalè, M.; Palermo, V.; Navacchia, M. L.; Melucci, M. Graphene oxide doped polysulfone membrane adsorbents for the removal of organic contaminants from water. *Chem. Eng. J.* **2017**, *326*, 130–140.
- (32) Ihsanullah; Abbas, A.; Al-Amer, A. M.; Laoui, T.; Al-Marri, M. J.; Nasser, M. S.; Khraisheh, M.; Ali Atieh, M. Heavy metal removal from aqueous solution by advanced carbon nanotubes: Critical review of adsorption applications. *Sep. Purif. Technol.* **2016**, *157*, 141–161.
- (33) Fu, F.; Wang, Q. Removal of heavy metal ions from wastewaters: A review. *J. Environ. Manage.* **2011**, *92*, 407–418.
- (34) Qu, X.; Alvarez, P. J. J.; Li, Q. Applications of nanotechnology in water and wastewater treatment. *Water Res.* **2013**, *47*, 3931–3946.
- (35) Yang, L.; Phua, S. L.; Teo, J. K. H.; Toh, C. L.; Lau, S. K.; Ma, J.; Lu, X. A Biomimetic Approach to Enhancing Interfacial Interactions: Polydopamine-Coated Clay as Reinforcement for Epoxy Resin. *ACS Appl. Mater. Interfaces* **2011**, *3*, 3026–3032.
- (36) Hopkins, J.; Badyal, J. P. S. XPS and atomic force microscopy of plasma-treated polysulfone. *J. Polym. Sci., Part A: Polym. Chem.* **1996**, *34*, 1385–1393.
- (37) Clark, M. B.; Gardella, J. A.; Schultz, T. M.; Patil, D. G.; Salvati, L. Solid-state analysis of eumelanin biopolymers by electron spectroscopy for chemical analysis. *Anal. Chem.* **1990**, *62*, 949–956.
- (38) Gao, J.; Lei, H.; Han, Z.; Shi, Q.; Chen, Y.; Jiang, Y. Dopamine functionalized tannic-acid-templated mesoporous silica nanoparticles as a new sorbent for the efficient removal of Cu²⁺ from aqueous solution. *Sci. Rep.* **2017**, *7*, 45215.
- (39) Eastoe, J.; Dalton, J. S. Dynamic surface tension and adsorption mechanisms of surfactants at the air–water interface. *Adv. Colloid Interface Sci.* **2000**, *85*, 103–144.
- (40) Skopp, J. Derivation of the Freundlich Adsorption Isotherm from Kinetics. *J. Chem. Educ.* **2009**, *86*, 1341.
- (41) Dubinin, M. M.; Zaverina, E. D.; Radushkevich, L. V. Sorption and Structure of Active Carbons I. Adsorption of Organic Vapors. *Zh. Fiz. Khim.* **1947**, *21*, 1351–1362.
- (42) Chen, H.; Zhao, J.; Wu, J.; Dai, G. Isotherm, thermodynamic, kinetics and adsorption mechanism studies of methyl orange by surfactant modified silkworm exuviae. *J. Hazard. Mater.* **2011**, *192*, 246–254.
- (43) Ju, K.-Y.; Lee, Y.; Lee, S.; Park, S. B.; Lee, J.-K. Bioinspired Polymerization of Dopamine to Generate Melanin-Like Nanoparticles Having an Excellent Free-Radical-Scavenging Property. *Biomacromolecules* **2011**, *12*, 625–632.